

ULTRA-CLOSE ENCOUNTERS OF STARS WITH MASSIVE BLACK HOLES:
TIDAL DISRUPTION EVENTS WITH PROMPT HYPERACCRETIONCHRISTOPHER EVANS¹, PABLO LAGUNA¹, AND MICHAEL ERACLEOUS^{2,1}*Draft version December 30, 2022*

ABSTRACT

A bright flare from a galactic nucleus followed at late times by a $t^{-5/3}$ decay in luminosity is often considered to be the signature of a tidal disruption of a star by a massive black hole. The flare and afterglow are produced when the stream of stellar debris released by the disruption returns to the vicinity of the black hole, self-intersects, and eventually forms an accretion disk or torus. In the canonical scenario of a solar-type star disrupted by a $10^6 M_\odot$ black hole, the time between the disruption of the star and the formation of the accretion torus could be years. We present fully general relativistic simulations of a new class of tidal disruption events involving ultra-close encounters of solar-type stars with intermediate mass black holes. In these encounters, a thick disk forms promptly after disruption, on timescales of hours. After a brief initial flare, the accretion rate remains steady and highly super-Eddington for a few days at $\sim 10^2 M_\odot \text{ yr}^{-1}$.

Subject headings: black holes, accretion

1. INTRODUCTION

In the transient astronomical sky, observations of tidal disruption events (TDEs) have the potential to unveil the presence of super-massive black holes (BHs) at the centers of galaxies. In galaxies with quiescent BHs specifically, accretion-powered nuclear activity is absent and thus TDE signatures are, in principle, readily identifiable. The observational evidence for TDEs is rapidly accumulating (for recent examples, see Gezari et al. 2012, 2009, 2006; van Velzen et al. 2011; Donato et al. 2014; Levan et al. 2011; Cenko et al. 2012; Chornock et al. 2014; Arcavi et al. 2014; Maksym et al. 2010, 2013). A variety of theoretical scenarios have been considered to explain the recent observations, ranging from the traditional case of a disrupted main-sequence star (e.g., Strubbe & Quataert 2009, 2011), to more exotic events involving the total or partial disruption of evolved stars such as a white-dwarfs (e.g., Clausen & Eracleous 2011; Krolik & Piran 2011), red-giants (e.g., Davies & King 2005; Bogdanović et al. 2014), horizontal branch stars (e.g., Clausen et al. 2012), and even super-Jupiters (e.g., Nikolajuk & Walter 2013). Of particular interest are the theoretical models predicting ignition (e.g., Rosswog et al. 2009) or the amplification of magnetic fields to launch relativistic jets (e.g., Giannios & Metzger 2011; Shcherbakov et al. 2013; Coughlin & Begelman 2014; Tchekhovskoy et al. 2014; Kelley et al. 2014).

As the number of putative TDE observations grows, simulations that expand the parameter space are needed to interpret the wealth of observational data. This is the premise behind the present study. We have identified a region of TDE parameter space yielding prompt hyper-accretion and torus formation.

TDE modeling was pioneered by Rees (1988), Phin-

ney (1989), and Evans & Kochanek (1989). These studies were first in pointing out that, for the most likely scenario of the disruption of a main-sequence star by a $10^{6-7} M_\odot$ BH, an UV/X-ray flare followed by a $t^{-5/3}$ decay in luminosity should be expected. The flare and afterglow decay are produced by the accretion of bound stellar debris as it returns to the neighborhood of the BH. In particular, the $t^{-5/3}$ decay was singled-out as a ubiquitous signature for the presence of massive BHs. Subsequent studies have incorporated detailed micro-physics (see Lodato et al. 2009; Guillochon & Ramirez-Ruiz 2013; Rosswog et al. 2009, for recent examples), considered a wider variety of stellar objects, such as white-dwarfs and red-giants (Shcherbakov et al. 2013; Haas et al. 2012; Kobayashi et al. 2004; Rosswog et al. 2009; Bogdanović et al. 2014), covered longer dynamical times (Guillochon et al. 2009), and included better descriptions of gravity for ultra-close encounters (Laguna et al. 1993; Rosswog 2010; Cheng & Bogdanović 2014).

A challenging aspect of TDE studies is the inherent difficulty in modeling the formation of the accretion disk from the bound stellar debris (Shen & Matzner 2014; Coughlin & Begelman 2014; Cannizzo 1992; Cannizzo et al. 1990). The complication arises because, in canonical TDEs, the time between the disruption of the star and the formation of the accretion disk amounts to several orbital periods of the stellar debris that are in highly eccentric orbits. This translates into years for a solar-type star disrupted by a $10^6 M_\odot$ BH. For reference, numerical simulations in these cases cover at most a few tens of hours.

In a series of very recent papers, circularization of the returning debris is addressed with a variety of methods. Through hydrodynamic simulations, Shiohara et al. (2015) find that the debris circularizes at a larger radius than previously thought and that the accumulation of mass in the ensuing ring is fairly slow (the characteristic time scale is several times the orbital period of the most tightly bound debris). Guillochon & Ramirez-Ruiz (2015) consider the self-intersection of thin post-

plaguna@gatech.edu

¹Center for Relativistic Astrophysics and School of Physics
Georgia Institute of Technology, Atlanta, GA 30332²Department of Astronomy & Astrophysics and Institute for
Gravitation and the Cosmos, The Pennsylvania State University,
University Park, PA 16802

disruption streams for an ensemble of events and conclude that streams *typically* self-intersect at large distances from the BH, leading to a long viscous time and an extensive delay before the onset of rapid accretion. Bonnerot et al. (2015) and Hayasaki et al. (2015) carry out simulations using smooth-particle hydrodynamics and point out the importance of cooling on the rate of circularization of the debris; their general conclusion is that efficient cooling leads to very long circularization time scales, hence a delay in the onset of accretion. The picture emerging from the above studies is that, although accretion could be prompt under the right conditions, it is likely that the onset of accretion is delayed by an appreciable amount of time, perhaps of order a year.

Our study introduces examples of a new class of TDEs, for which a puffed disk or torus forms promptly after disruption. Furthermore, the BH accretes at a steady and highly super-Eddington rate of about $10^2 M_\odot \text{ yr}^{-1}$. This highly super-Eddington rate resembles those found by Coughlin & Begelman (2014), whose treatment does not include radiative diffusion, suggesting that radiative diffusion is inefficient in cooling the disk. The TDEs in our study involve ultra-close encounters between low mass ($0.57 - 1 M_\odot$) stars and a $10^5 M_\odot$ BH. The simulations fully account for general relativistic effects, including those from the spin of the BH. In these ultra-close encounters, the star is effectively disrupted as it arrives at periastris, with the tidal debris plunging into the BH almost instantaneously (on the timescale of one orbital period). Moreover, as a result of the extreme proximity of the debris to the BH, general relativistic precession is very efficient in circularizing stellar material to form an expanding torus that engulfs the BH. The inner material in the torus spirals into the BH and is accreted at a constant rate.

2. TIDAL DISRUPTIONS AT A GLANCE

A star of mass M_* and radius R_* approaching a BH of mass M_h , likely in a highly eccentric or parabolic orbit (Rees 1988; Magorrian & Tremaine 1999; Hayasaki et al. 2012), will be disrupted by tidal forces if the star wanders near the BH within a distance R_t , called the *tidal radius*, given approximately by

$$R_t \equiv R_* \left(\frac{M_h}{M_*} \right)^{1/3}. \quad (1)$$

Denoting the distance of closest approach to the BH as R_p , it is customary to characterize the strength of a TDE encounter by the *penetration factor* β , which is defined as

$$\beta \equiv \frac{R_t}{R_p} = \frac{R_*}{R_p} \left(\frac{M_h}{M_*} \right)^{1/3}. \quad (2)$$

The fourth length scale in the problem, in addition to R_* , R_t and R_p , is the gravitational radius $R_g = G M_h / c^2$, which is equal to half the horizon radius for a non-spinning BH and the full horizon radius for a maximally rotating BH.

Given R_* , R_t , R_p and R_g , it is useful to identify the domain of astrophysical relevance of TDEs, as first suggested by Luminet & Pichon (1989). One representation of this domain is a triangle in the β vs M_h diagram as shown in Figure 1. Interpreting β in Eq. (2) as a function

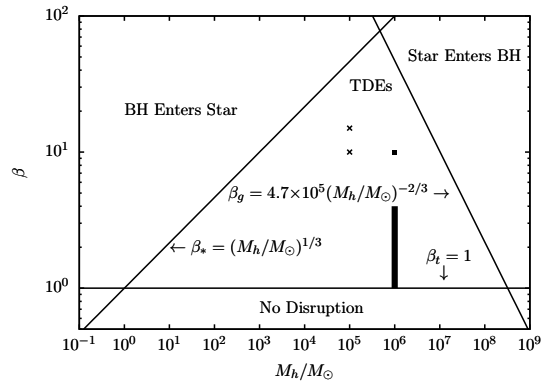


FIG. 1.— Domain of astrophysical relevance of tidal disruptions for a main-sequence star with mass $M_* = M_\odot$ and radius $R_* = R_\odot$. The thick vertical line denotes canonical TDEs. The square point shows the ultra-close TDE from Laguna et al. (1993) and crosses those in the present study.

of R_p clarifies the demarcations between different regions of parameter space. The base of the triangle is $R_p = R_t$, i.e. $\beta_t \equiv \beta(R_t) = 1$. Below this line ($R_p > R_t$) there is no disruption. The left side of the triangle is the line obtained by setting $R_p = R_*$; that is,

$$\beta_* \equiv \beta(R_*) = \left(\frac{M_h}{M_*} \right)^{1/3}. \quad (3)$$

To the left of this line ($R_p < R_*$) lie very close encounters where *the BH enters the star* in the process of disrupting it. The process has many similarities to the high-speed collisions of stellar-mass BHs and red giants as studied by Dale et al. (2009). Finally, the right side of the triangle is the line when $R_p = R_g$; that is,

$$\beta_g \equiv \beta(R_g) = \frac{R_*}{G M_h / c^2} \left(\frac{M_h}{M_*} \right)^{-2/3}. \quad (4)$$

To the right of this line ($R_p < R_g$) are events where the *star enters the BH* before it is disrupted.

According to Figure 1, for a solar-type star ($M_* = M_\odot$ and $R_* = R_\odot$), the maximum BH mass to disrupt the star is $M_h = 3.2 \times 10^8 M_\odot$. Moreover, the maximum penetration factor with disruption is $\beta = 78$, which involves a $M_h = 4.7 \times 10^5 M_\odot$ BH. The edges of the triangle of astrophysical relevance are, of course, not sharp due to variations in the definition of relevant length scales arising from the spin of the BH, the space-time curvature in the neighborhood of the BH, and the internal structure of the star.

After periastris passage the debris spreads as it recedes from the BH, with roughly half of the material remaining unbound. This unbound material could potentially reprocess the radiation emerging from the neighborhood of the BH and produce optical emission lines (Strubbe & Quataert 2009). The remaining bound material returns to the BH on the orbital timescale. The most bound material has specific binding energy e_{\min} , which is given by the change of the gravitational potential across the size of debris stream, $\Delta R_* = \xi R_*$, with ξ a deformation factor (Evans & Kochanek 1989); that is,

$$e_{\min} \simeq -\frac{G M_h}{R_p} \left(\frac{\Delta R_*}{R_p} \right) \simeq -G \beta^2 \xi M_*^{2/3} R_*^{-1} M_h^{1/3}. \quad (5)$$

With e_{\min} at hand, the characteristic fallback time for the most tightly bound material to return to the BH is

$$t_{\min} \simeq 2\pi \frac{G M_h}{(2|e_{\min}|)^{3/2}} \simeq \frac{\pi}{\sqrt{2G}} \beta^{-3} \xi^{-3/2} R_*^{3/2} M_*^{-1} M_h^{1/2}. \quad (6)$$

An estimate of the debris return at late times is obtained from the Keplerian relation

$$\frac{de}{dt} = \frac{1}{3} (2\pi G M_h)^{2/3} t^{-5/3} \quad (7)$$

and the mass per specific binding energy

$$\frac{dM_h}{de} \simeq \frac{M_*}{2|e_{\min}|} \simeq \frac{M_*}{t_{\min}^{-2/3}} \frac{1}{(2\pi G M_h)^{2/3}}, \quad (8)$$

which is assumed to be roughly constant. Therefore,

$$\dot{M}_h \equiv \frac{dM_h}{dt} = \frac{dM_h}{de} \frac{de}{dt} \simeq \dot{M}_{\max} \left(\frac{t}{t_{\min}} \right)^{-5/3}. \quad (9)$$

with $\dot{M}_{\max} \equiv M_*/(3t_{\min})$. The power-law decay of $t^{-5/3}$ in Eq. (9) is considered to be a ubiquitous property of TDEs as long as the mass per unit binding energy of the debris is approximately constant (Rees 1988; Evans & Kochanek 1989; Laguna et al. 1993; Rosswog et al. 2009). Slight departures from this power-law have been found close to the peak accretion rate as a result of the equation of state of the star (Lodato et al. 2009) or effects from the spin of the massive BH (Haas et al. 2012).

In the case of a TDE with $M_* = M_\odot$, $R_* = R_\odot$ and $M_h = 10^6 M_\odot$,

$$t_{\min} \simeq 0.11 \beta^{-3} \xi^{-3/2} r_*^{3/2} m_*^{-1} M_6^{1/2} \text{ yr}, \quad (10)$$

and

$$\dot{M}_{\max} \simeq 0.3 \beta^3 \xi^{3/2} r_*^{-3/2} m_*^2 M_6^{-1/2} M_\odot \text{ yr}^{-1}, \quad (11)$$

where $M_6 \equiv M_h/10^6 M_\odot$, $r_* \equiv R_*/R_\odot$ and $m_* \equiv M_*/M_\odot$. For comparison, the Eddington accretion rate in this situation is $\dot{M}_{\text{Edd}} = 0.02 M_6 M_\odot \text{ yr}^{-1}$ (assuming 10% efficiency).

3. NEW TDE REGIME

We are interested in TDEs with penetration factors $\beta = 10$ and 15, involving a BH with mass $M_h = 10^5 M_\odot$. They are denoted by crosses in Figure 1 and are closer to the *BH-enters-star* boundary than the “canonical” scenarios of $\beta = \text{few}$ and $M_h = 10^6 M_\odot$, which are denoted by a thick vertical line in Figure 1. In the same figure, the square point shows the ultra-close TDE from Laguna et al. (1993). We consider non-spinning BHs and BHs with spin $a/M_h = \pm 0.65$. The sign denotes whether the spin of the BH is aligned (plus) or anti-aligned (minus) with the orbital angular momentum of the star. The disruptions involve main-sequence type stars with masses

$M_* = 1 M_\odot$ and $0.57 M_\odot$, modeled as polytropes with index $\Gamma = 4/3$ and injected in parabolic orbits. Table 1 provides the parameters of the simulations: the penetration factor β , the BH spin parameter a , and the mass of the star M_* . The simulations fully account for general relativistic effects. To this end, we use our numerical relativity infrastructure Maya, used also in our previous general relativistic TDE studies (Haas et al. 2012).

In general terms, the TDEs studied here involve stars comparable in size to the BH, $R_* \simeq 4.7 M_5^{-1} r_* R_g$, periastron distances of about

$$R_p \simeq 4.64 \beta_{10}^{-1} M_5^{1/3} m_*^{-1/3} R_*, \quad (12)$$

and tidal radius

$$R_t \simeq 218 M_5^{-2/3} m_*^{-1/3} r_* R_g, \quad (13)$$

where $M_5 \equiv M_h/10^5 M_\odot$ and $\beta_{10} \equiv \beta/10$. Although the value of R_p above suggests that the star could potentially swing by the BH without the BH entering the star, the combination of large penetration factors and general relativistic effects produce an outcome dramatically different from the situations involving moderate penetrations and $10^6 M_\odot$ mass BHs (next section).

With $\beta \geq 10$ and intermediate mass BHs, the star will be effectively disrupted and stretched to a few times its original size by the time it reaches periastron passage. A deformation factor $\xi \simeq 4$ was found to be common in our simulations. Therefore, from Eqs. (6) and (9)

$$t_{\min} \simeq 137 \beta_{10}^{-3} \xi_4^{-3/2} r_*^{3/2} m_*^{-1} M_5^{1/2} \text{ s}, \quad (14)$$

and

$$\dot{M}_{\max} \simeq 9.6 \times 10^3 \beta_{10}^3 \xi_4^{3/2} r_*^{-3/2} m_*^2 M_5^{-1/2} M_\odot \text{ yr}^{-1}, \quad (15)$$

where $\xi_4 = \xi/4$. For reference, the Eddington accretion rate in this case is $\dot{M}_{\text{Edd}} = 0.002 M_5 M_\odot \text{ yr}^{-1}$. Our simulations show that $\dot{M}_{\max} \sim 10^4 M_\odot \text{ yr}^{-1}$ and $t_{\min} \sim 25 \text{ s}$. This time-scale is comparable to the circular orbital period of the most bound material:

$$P_{\text{circ}} = 2\pi \sqrt{\frac{(R_p - \Delta R)^3}{G M_h}} \simeq 316 (1 - \Delta R/R_p)^{3/2} \beta_{10}^{-3/2} r_*^{3/2} m_*^{-1/2} \text{ s} \simeq 16.5 \beta_{10}^{-3/2} r_*^{3/2} m_*^{-1/2} \text{ s}, \quad (16)$$

where $\Delta R/R_p \simeq 0.86 \xi_4 \beta_{10} m_*^{1/3} M_5^{1/3}$.

4. ANATOMY OF A DISRUPTION

We focus this discussion chiefly on the accretion rates onto the BH. Figure 2 shows the accretion rates of tidal debris through the BH horizon. The time axis is such that $t = 0 \text{ s}$ denotes periastron passage. Three distinct accretion epochs or stages are identifiable in most of the cases.

The first phase is a narrow spike or flare in the accretion rate. The spike is due to the portion of the stellar debris that immediately plunges into the BH. An estimate of this accretion rate is given by

$$\dot{M}_h \sim A_h \rho_\infty v_\infty \sim 10^4 \beta_{10}^{1/2} M_5^{7/3} m_*^{7/6} r_*^{-7/2} M_\odot \text{ yr}^{-1}, \quad (17)$$

TABLE 1
SIMULATION PARAMETERS AND ACCRETION RATES.

Run	β	a/M_h	M_*/M_\odot	$\dot{M}_{\max} (M_\odot \text{ yr}^{-1})$	$\dot{M}_{\text{late}} (M_\odot \text{ yr}^{-1})$
$\beta_{10} S_0 M_1$	10	0	1	3.6×10^2	1.0×10^3
$\beta_{10} S_{0.65} M_1$	10	0.65	1	1.0×10^4	7.5×10^2
$\beta_{10} S_{-0.65} M_1$	10	-0.65	1	1.2×10^5	2.0×10^2
$\beta_{10} S_0 M_{0.57}$	10	0	0.57	3.5×10^2	1.0×10^2
$\beta_{10} S_{0.65} M_{0.57}$	10	0.65	0.57	7.6×10^3	4.0×10^2
$\beta_{10} S_{-0.65} M_{0.57}$	10	-0.65	0.57	7.9×10^4	3.0×10^2
$\beta_{15} S_0 M_{0.57}$	15	0	0.57	2.0×10^4	4.0×10^2
$\beta_{15} S_{0.65} M_{0.57}$	15	0.65	0.57	8.8×10^4	3.5×10^2
$\beta_{15} S_{-0.65} M_{0.57}$	15	-0.65	0.57	3.8×10^5	2.0×10^2

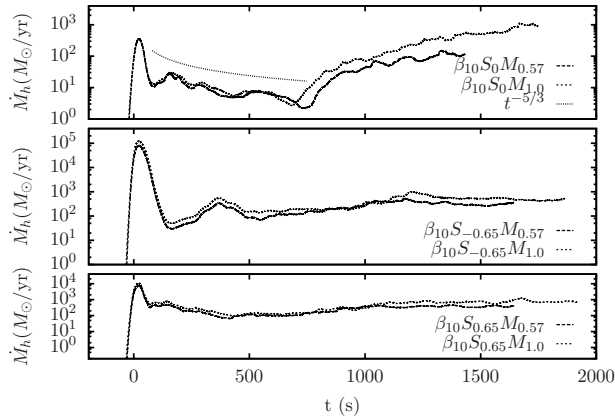


FIG. 2.— BH accretion rate as a function of time for penetration factor $\beta = 10$. The cases in each panel are grouped by the spin parameter of the BH in order to assess the effect of the mass of the star. For reference in the top panel a dashed line denotes a $t^{-5/3}$ decay.

where we have used $A_h \sim 4\pi R_g^2$, $v_\infty \sim (GM_h/R_p)^{1/2}$ and $\rho_\infty \sim M_*/(4\pi R_*^3/3)$. This estimate is consistent with the values for \dot{M}_{\max} reported in Table 1.

The next stage following the accretion flare is a decay phase, which for the simulations involving a non-spinning BH as seen in Figure 2 (top panel), loosely resembles a $t^{-5/3}$ law (dashed line in top panel). The duration and the presence of power-law decay seem to depend on the spin of the BH and the penetration factor β .

Finally, as new material returns to the BH, it circularizes and forms an accretion torus on a timescale of $\sim 10 t_{\min} \sim 1,400$ s (Evans & Kochanek 1989), with the accretion eventually reaching steady state at about $\dot{M}_{\text{late}} \sim 10^2 M_\odot \text{ yr}^{-1}$, as noted in the last column of Table 1.

5. SIMULATION RESULTS

We report results from nine simulations, with parameters summarized in Table 1. To illustrate the effect of the mass of the star, Figure 2 shows the BH accretion rate, grouping the cases with the same BH spin parameter and penetration factor. Notice that the accretion rate seems to be insensitive to the mass of the star. Perhaps the only case with noticeable differences is that of vanishing BH spin. We will thus focus the discussion on the star with mass $M_* = 0.57 M_\odot$ since we have a wider variety of simulations for this star.

In Figure 3, we organize the runs according to the pen-

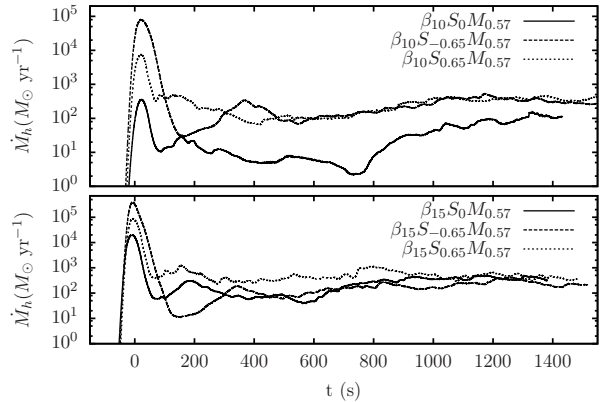


FIG. 3.— BH accretion rate as a function of time for penetration factor $\beta = 10$ (top panel) and $\beta = 15$ (bottom panel) for the $M_* = 0.57 M_\odot$ cases.

etration factor, with $\beta = 10$ in the top panel and $\beta = 15$ in the bottom panel. Notice that the peak accretion rate of the flare is higher if the BH is spinning. Interestingly, the case with a counter-rotating orbit (i.e. BH spin anti-aligned with the orbital angular momentum) yields the largest peak accretion rate. For the $\beta = 10$ simulations, the post-flare accretion rate depends on the BH spin magnitude but not its orientation, which is consistent with similar findings for the steady-state, subsonic accretion onto a moving BH (Petrich et al. 1988). The late-time accretion rate seems to increase with the spin of the BH. Another difference between the $a/M_h = 0$ and the $a/M_h = \pm 0.65$ cases is that for the latter, the time scale for flare decay is shorter; that is, the late constant accretion phase, which signals the formation of the torus, is reached after a couple of hundred seconds.

The corresponding $\beta = 15$ cases show that the spin of the BH does not play a role in determining the late-time, constant accretion rate. Furthermore, as with the $\beta = 10$ cases with spinning BHs, the constant accretion phase is reached within a few hundred seconds. For both the $\beta = 10$ and $\beta = 15$ cases, the late-time accretion rate is of the order of $10^2 M_\odot \text{ yr}^{-1}$.

In summary, given the parameters that we varied (M_* , a/M_h , β) and the region of parameter space that we explored, we found that the accretion rate is not very sensitive to M_* , and that the rate reached during the flare depends on both a/M_h and β . Furthermore, the late accretion rate for $\beta = 15$ is not sensitive to the spin of the BH, and for both penetration factors is approxi-

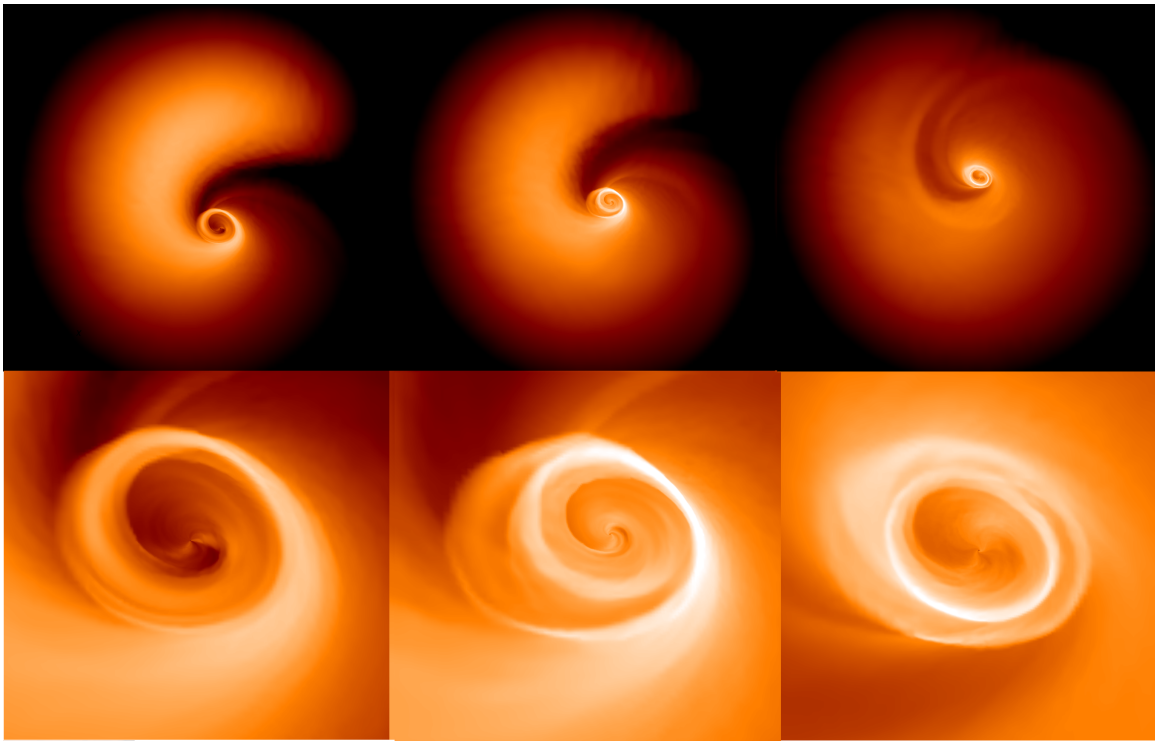


FIG. 4.— Snapshots of the density of the stellar debris at a time ~ 5.9 seconds after disruption. From left to right are the cases $\beta_{10}S_0M_{0.57}$, $\beta_{10}S_{0.65}M_{0.57}$ and $\beta_{15}S_{-0.65}M_{0.57}$, respectively.

mately $\dot{M}_h \sim 10^2 M_\odot \text{yr}^{-1}$. It is important to point out that with the exception of the cases with $\beta = 10$ and $a/M_h = 0, 0.65$ (top panel Figure 2), there are no hints of a $t^{-5/3}$ decay rate.

Figure 4 shows snapshots of the density of the stellar debris at ~ 5.9 s after the disruption. The top row shows the density in the orbital plane, and the bottom row close-ups of the corresponding snapshot in the top row. From left to right in Figure 4 are the cases $\beta_{10}S_0M_{0.57}$, $\beta_{10}S_{0.65}M_{0.57}$ and $\beta_{15}S_{-0.65}M_{0.57}$, respectively. Both the self-intersection of stellar debris and the consequent formation of the accretion torus are evident in these snapshots.

6. CONCLUSIONS

We presented a new class of TDEs showing prompt formation of an accretion torus after disruption and hyperaccretion. These TDEs involve ultra-close encounters with $M_h = 10^5 M_\odot$ BH. The accretion rates of tidal material are highly super-Eddington. Additionally, there is little evidence of a $t^{-5/3}$ decay in the accretion rate. This is likely due the strong influence of general relativistic effects in these ultra-close encounters. The late-time accretion rate, once the torus has formed, reaches an approximate steady-state and remains highly super-Eddington at $\dot{M}_{\text{late}} \sim 10^2 M_\odot \text{yr}^{-1}$. With this rate, the BH should be able to accrete the majority of the bound

tidal debris in just a few days. A word of caution is needed regarding the accretion rate quotes in this study. Our simulations did not include effects from radiation, which could potentially decrease the rates. However, it is not likely that radiation effects would diminish the rates enough to make them sub-Eddington, since the Eddington rate in these situations is $\dot{M}_{\text{Edd}} = 0.002 M_5 M_\odot \text{yr}^{-1}$ (assuming 10% efficiency).

In a subsequent study, we will expand the parameter space of our simulations and investigate the emission properties of the tidal debris. In light of the results of recent papers cited in the introduction regarding the circularization of post-disruption debris, it will be important to investigate further the role of shocks in heating and circularizing the debris as well as the overall role of cooling effects. Moreover, we will consider inclined orbits relative to the spin axis of the BH in order to compare our results with those of Shen & Matzner (2014). We are also interested in the possibility of amplification of magnetic fields and whether the class of TDEs in the present study could provide an explanation for jetted events, such as Swift J1644+57 (Burrows et al. 2011; Levan et al. 2011).

We thank Tamara Bogdanović for fruitful discussions and comments. M.E. is grateful to the Center Relativistic Astrophysics at Georgia Tech for their hospitality during the early phases of this work. This work was supported by NSF grants 1205864, 1212433, 1333360. Computations at XSEDE TG-PHY120016 and the Cygnus cluster at Georgia Tech.

REFERENCES

- Arcavi, I., Gal-Yam, A., Sullivan, M., Pan, Y.-C., Cenko, S. B., Horesh, A., Ofek, E. O., De Cia, A., Yan, L., Yang, C.-W., Howell, D. A., Tal, D., Kulkarni, S. R., Tendulkar, S. P., Tang, S., Xu, D., Sternberg, A., Cohen, J. G., Bloom, J. S., Nugent, P. E., Kasliwal, M. M., Perley, D. A., Quimby, R. M., Miller, A. A., Theissen, C. A., & Laher, R. R. 2014, *ApJ*, 793, 38
- Bogdanović, T., Cheng, R. M., & Amaro-Seoane, P. 2014, *ApJ*, 788, 99
- Bonnerot, C., Rossi, E. M., Lodato, G., & Price, D. J. 2015, ArXiv e-prints

- Burrows, D. N., Kennea, J. A., Ghisellini, G., Mangano, V., Zhang, B., Page, K. L., Eracleous, M., Romano, P., Sakamoto, T., Falcone, A. D., Osborne, J. P., Campana, S., Beardmore, A. P., Breeveld, A. A., Chester, M. M., Corbet, R., Covino, S., Cummings, J. R., D'Avanzo, P., D'Elia, V., Esposito, P., Evans, P. A., Fugazza, D., Gelbord, J. M., Hiroi, K., Holland, S. T., Huang, K. Y., Im, M., Israel, G., Jeon, Y., Jeon, Y.-B., Jun, H. D., Kawai, N., Kim, J. H., Krimm, H. A., Marshall, F. E., P. Mészáros, Negoro, H., Omodei, N., Park, W.-K., Perkins, J. S., Sugizaki, M., Sung, H.-I., Tagliaferri, G., Troja, E., Ueda, Y., Urata, Y., Usui, R., Antonelli, L. A., Barthelmy, S. D., Cusumano, G., Giommi, P., Melandri, A., Perri, M., Racusin, J. L., Sbarufatti, B., Siegel, M. H., & Gehrels, N. 2011, *Nature*, 476, 421
- Cannizzo, J. K. 1992, *ApJ*, 385, 94
- Cannizzo, J. K., Lee, H. M., & Goodman, J. 1990, *ApJ*, 351, 38
- Cenko, S. B., Krimm, H. A., Horesh, A., Rau, A., Frail, D. A., Kennea, J. A., Levan, A. J., Holland, S. T., Butler, N. R., Quimby, R. M., Bloom, J. S., Filippenko, A. V., Gal-Yam, A., Greiner, J., Kulkarni, S. R., Ofek, E. O., Olivares E., F., Schady, P., Silverman, J. M., Tanvir, N. R., & Xu, D. 2012, *Astrophysical Journal*, 753, 77
- Cheng, R. M. & Bogdanović, T. 2014, *Phys. Rev. D*, 90, 064020
- Chornock, R., Berger, E., Gezari, S., Zauderer, B. A., Rest, A., Chomiuk, L., Kamble, A., Soderberg, A. M., Czekala, I., Dittmann, J., Drout, M., Foley, R. J., Fong, W., Huber, M. E., Kirshner, R. P., Lawrence, A., Lunnan, R., Marion, G. H., Narayan, G., Riess, A. G., Roth, K. C., Sanders, N. E., Scolnic, D., Smartt, S. J., Smith, K., Stubbs, C. W., Tonry, J. L., Burgett, W. S., Chambers, K. C., Flewelling, H., Hodapp, K. W., Kaiser, N., Magnier, E. A., Martin, D. C., Neill, J. D., Price, P. A., & Wainscoat, R. 2014, *ApJ*, 780, 44
- Clausen, D. & Eracleous, M. 2011, *ApJ*, 726, 34
- Clausen, D., Sigurdsson, S., Eracleous, M., & Irwin, J. A. 2012, *MNRAS*, 424, 1268
- Coughlin, E. R. & Begelman, M. C. 2014, *ApJ*, 781, 82
- Dale, J. E., Davies, M. B., Church, R. P., & Freitag, M. 2009, *MNRAS*, 393, 1016
- Davies, M. B. & King, A. 2005, *ApJ*, 624, L25
- Donato, D., Cenko, S. B., Covino, S., Troja, E., Pursimo, T., Cheung, C. C., Fox, O., Kutyrev, A., Campana, S., Fugazza, D., Landt, H., & Butler, N. R. 2014, *ApJ*, 781, 59
- Evans, C. R. & Kochanek, C. S. 1989, *Astrophysical Journal Letters*, 346, L13
- Gezari, S., Chornock, R., Rest, A., Huber, M. E., Forster, K., Berger, E., Challis, P. J., Neill, J. D., Martin, D. C., Heckman, T., Lawrence, A., Norman, C., Narayan, G., Foley, R. J., Marion, G. H., Scolnic, D., Chomiuk, L., Soderberg, A., Smith, K., Kirshner, R. P., Riess, A. G., Smartt, S. J., Stubbs, C. W., Tonry, J. L., Wood-Vasey, W. M., Burgett, W. S., Chambers, K. C., Grav, T., Heasley, J. N., Kaiser, N., Kudritzki, R.-P., Magnier, E. A., Morgan, J. S., & Price, P. A. 2012, *Nature*, 485, 217
- Gezari, S., Heckman, T., Cenko, S. B., Eracleous, M., Forster, K., Gonçalves, T. S., Martin, D. C., Morrissey, P., Neff, S. G., Seibert, M., Schiminovich, D., & Wyder, T. K. 2009, *ApJ*, 698, 1367
- Gezari, S., Martin, D. C., Milliard, B., Basa, S., Halpern, J. P., Forster, K., Friedman, P. G., Morrissey, P., Neff, S. G., Schiminovich, D., Seibert, M., Small, T., & Wyder, T. K. 2006, *ApJ*, 653, L25
- Giannios, D. & Metzger, B. D. 2011, *MNRAS*, 416, 2102
- Guillochon, J. & Ramirez-Ruiz, E. 2013, *ApJ*, 767, 25
- . 2015, ArXiv e-prints
- Guillochon, J., Ramirez-Ruiz, E., Rosswog, S., & Kasen, D. 2009, *ApJ*, 705, 844
- Haas, R., Shcherbakov, R. V., Bode, T., & Laguna, P. 2012, *ApJ*, 749, 117
- Hayasaki, K., Stone, N., & Loeb, A. 2012, in *European Physical Journal Web of Conferences*, Vol. 39, European Physical Journal Web of Conferences, 1004
- Hayasaki, K., Stone, N. C., & Loeb, A. 2015, ArXiv e-prints
- Kelley, L. Z., Tchekhovskoy, A., & Narayan, R. 2014, *MNRAS*, 445, 3919
- Kobayashi, S., Laguna, P., Phinney, E. S., & Mészáros, P. 2004, *ApJ*, 615, 855
- Krolik, J. H. & Piran, T. 2011, *ApJ*, 743, 134
- Laguna, P., Miller, W. A., Zurek, W. H., & Davies, M. B. 1993, *ApJ*, 410, L83
- Levan, A. J., Tanvir, N. R., Cenko, S. B., Perley, D. A., Wiersema, K., Bloom, J. S., Fruchter, A. S., Postigo, A. d. U., O'Brien, P. T., Butler, N., van der Horst, A. J., Leloudas, G., Morgan, A. N., Misra, K., Bower, G. C., Farihi, J., Tunnicliffe, R. L., Modjaz, M., Silverman, J. M., Hjorth, J., Thöne, C., Cucchiara, A., Cerón, J. M. C., Castro-Tirado, A. J., Arnold, J. A., Bremer, M., Brodie, J. P., Carroll, T., Cooper, M. C., Curran, P. A., Cutri, R. M., Ehle, J., Forbes, D., Fynbo, J., Gorosabel, J., Graham, J., Hoffman, D. I., Guziy, S., Jakobsson, P., Kamble, A., Kerr, T., Kasliwal, M. M., Kouveliotou, C., Kocevski, D., Law, N. M., Nugent, P. E., Ofek, E. O., Poznanski, D., Quimby, R. M., Rol, E., Romanowsky, A. J., Sánchez-Ramírez, R., Schulze, S., Singh, N., van Spaandonk, L., Starling, R. L. C., Strom, R. G., Tello, J. C., Vaduvescu, O., Wheatley, P. J., Wijers, R. A. M. J., Winters, J. M., & Xu, D. 2011, *Science*, 333, 199
- Lodato, G., King, A. R., & Pringle, J. E. 2009, *Monthly Notices of the Royal Astronomical Society*, 392, 332
- Luminet, J.-P. & Pichon, B. 1989, *A&A*, 209, 103
- Magorrian, J. & Tremaine, S. 1999, *MNRAS*, 309, 447
- Maksym, W. P., Ulmer, M. P., & Eracleous, M. 2010, *ApJ*, 722, 1035
- Maksym, W. P., Ulmer, M. P., Eracleous, M. C., Guennou, L., & Ho, L. C. 2013, *MNRAS*, 435, 1904
- Nikolajuk, M. & Walter, R. 2013, *A&A*, 552, A75
- Petrich, L. I., Shapiro, S. L., & Teukolsky, S. A. 1988, *Phys. Rev. Lett.*, 60, 1781
- Phinney, E. S. 1989, in *IAU Symposium*, Vol. 136, *The Center of the Galaxy*, ed. M. Morris, 543
- Rees, M. J. 1988, *Nature*, 333, 523
- Rosswog, S. 2010, *Classical and Quantum Gravity*, 27, 114108
- Rosswog, S., Ramirez-Ruiz, E., & Hix, W. R. 2009, *ApJ*, 695, 404
- Shcherbakov, R. V., Pe'er, A., Reynolds, C. S., Haas, R., Bode, T., & Laguna, P. 2013, *ApJ*, 769, 85
- Shen, R.-F. & Matzner, C. D. 2014, *ApJ*, 784, 87
- Shiokawa, H., Krolik, J. H., Cheng, R. M., Piran, T., & Noble, S. C. 2015, ArXiv e-prints
- Strubbe, L. E. & Quataert, E. 2009, *MNRAS*, 400, 2070
- . 2011, *M.N.R.A.S.*, 415, 168
- Tchekhovskoy, A., Metzger, B. D., Giannios, D., & Kelley, L. Z. 2014, *MNRAS*, 437, 2744
- van Velzen, S., Farrar, G. R., Gezari, S., Morrell, N., Zaritsky, D., Östman, L., Smith, M., Gelfand, J., & Drake, A. J. 2011, *ApJ*, 741, 73